Development of an advanced cladding mechanical model and its application for thermal hydraulics coupled failure analysis of SiC LWR fuel cladding during LBLOCA

Hyuntaek Rho, Youho Lee*

rho96@snu.ac.kr
leeyouho@snu.ac.kr

Seoul National University
Nuclear Fuel Materials and Safety Laboratory

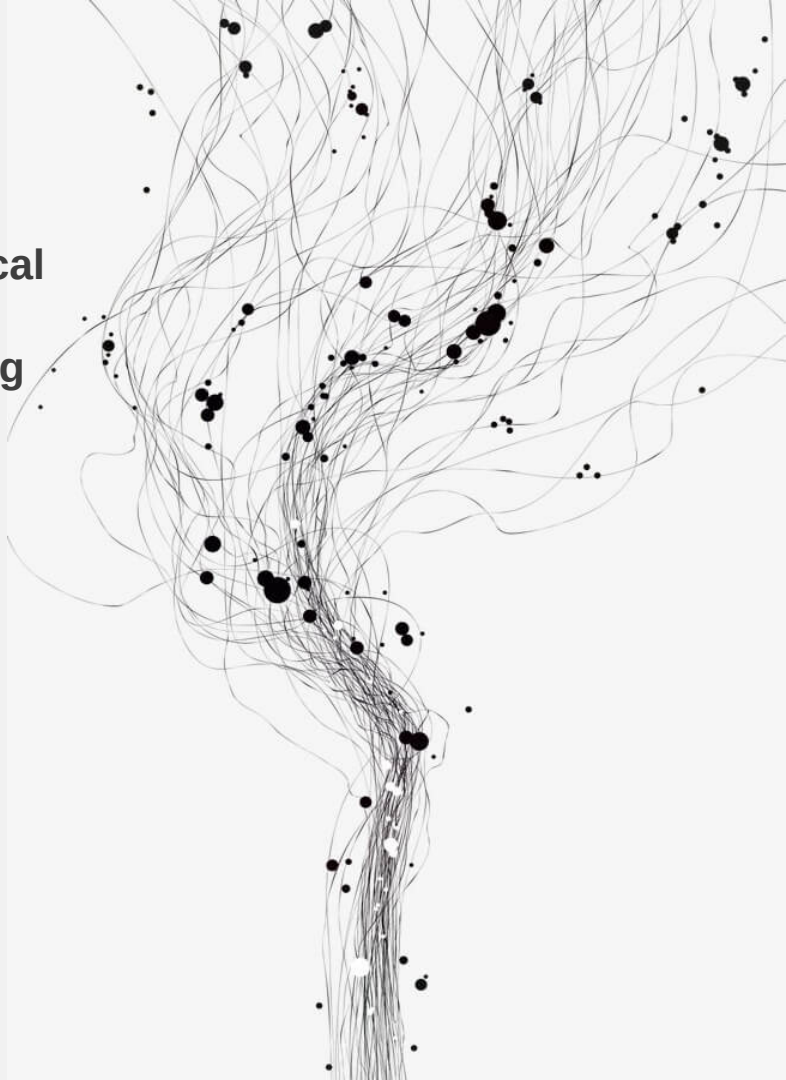

목차

CONTENTS

Introduction

- Code development
- SiC cladding

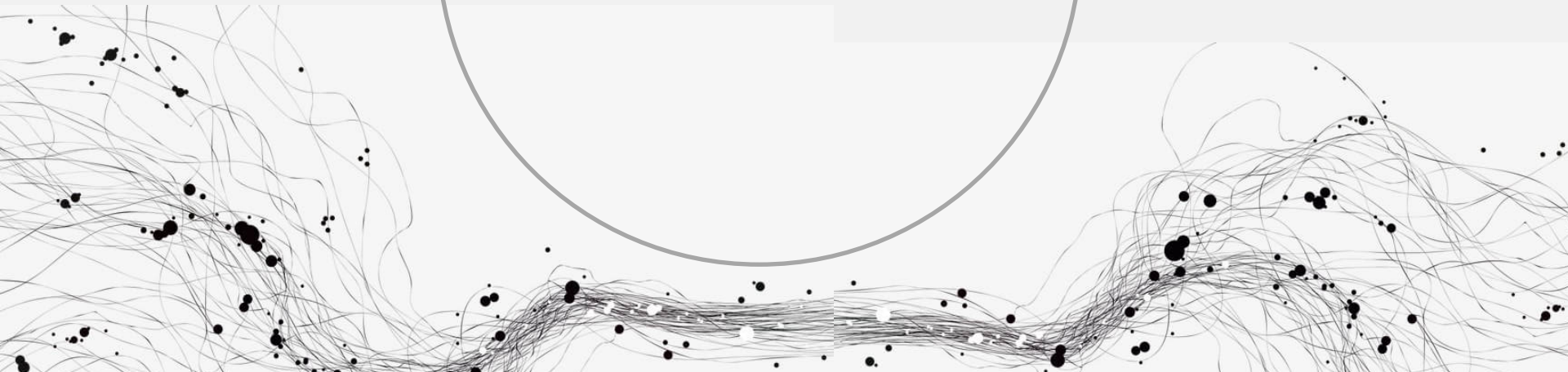

Code development

Introduction

Previous mechanical model	Advanced mechanical model
1-D FDM - Fast but doesn't consider axial interaction - Easy to analyze entire cladding size - Applicable only when the shape of cladding is not significantly modified 2-D FEM - Reliable result - Hard to analyze entire cladding size	2-D FDM - Fast and consider axial interaction - Easy to analyze entire cladding size - Applicable only when the shape of cladding is not significantly modified

SiC cladding

Introduction

- SiC has a melting point of 2730°C and maintains strength even at high temperature of 1500°C.

- SiC is chemically stable and has four orders of magnitude lower corrosion rate than zircaloy for steam at high temperatures.

- As materials for nuclear grade SiC cladding, Chemical Vapor Deposited (CVD) monolithic SiC (mSiC) and Chemical Vapor Infiltration (CVI) SiCf/SiC Ceramic Matrix Composite (CMC) are used.

- CVD-SiC cannot be used alone for cladding because it has brittle nature due to the characteristics of ceramics and shows statistical failure behavior. Therefore, it is necessary to use CMC with pseudo-ductility to compensate for this.

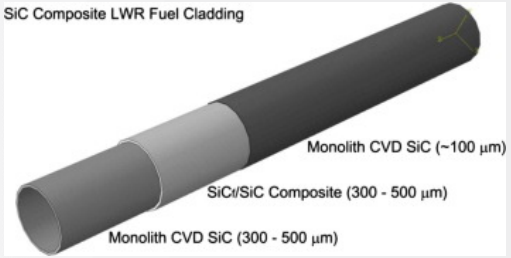

Triple-layer SiC cladding

SiC fiber reinforced cladding

Code Development

- Derivation of equations
- Differentiation
- Plastic & creep model
- Boundary conditions
- Verification

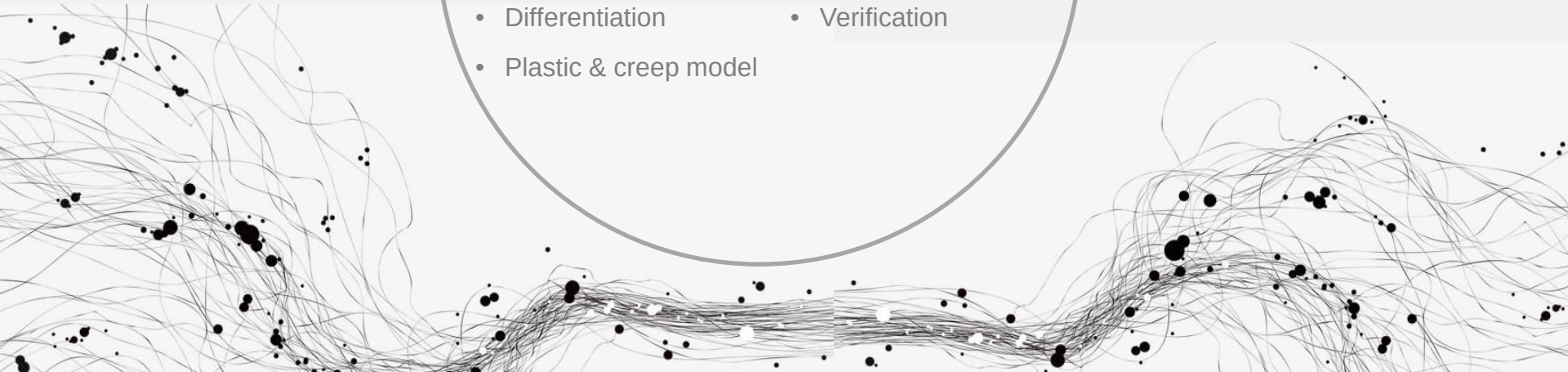

Derivation of equations

Code development

Equilibrium Equation

$$\frac{\partial \sigma_{rr}}{\partial r} + \frac{\partial \tau_{rz}}{\partial z} + \frac{\sigma_{rr} - \sigma_{\theta\theta}}{r} = 0 \quad (1)$$

$$\frac{\partial \sigma_{zz}}{\partial z} + \frac{\partial \tau_{rz}}{\partial r} + \frac{\tau_{zr}}{r} = 0 \quad (2)$$

Constitutive Equation

$$\epsilon_{rr} = \frac{\sigma_{rr}}{E_{rr}} - \frac{V_{\theta r}\sigma_{\theta\theta}}{E_{\theta\theta}} - \frac{V_{zr}\sigma_{zz}}{E_{zz}} + \alpha_{rr}\Delta T + S_{rr} \quad (3)$$

$$\epsilon_{\theta\theta} = \frac{\sigma_{\theta\theta}}{E_{\theta\theta}} - \frac{V_{z\theta}\sigma_{zz}}{E_{zz}} - \frac{V_{r\theta}\sigma_{rr}}{E_{rr}} + \alpha_{\theta\theta}\Delta T + S_{\theta\theta} \quad (4)$$

$$\epsilon_{zz} = \frac{\sigma_{zz}}{E_{zz}} - \frac{V_{rz}\sigma_{rr}}{E_{rr}} - \frac{V_{\theta z}\sigma_{\theta\theta}}{E_{\theta\theta}} + \alpha_{zz}\Delta T + S_{zz} \quad (5)$$

$$\gamma_{rz} = \frac{\tau_{rz}}{G} \quad (6)$$

Deformation(kinematic) Relations

$$\epsilon_{rr} = \frac{\partial u_r}{\partial r} \quad (7)$$

$$\epsilon_{\theta\theta} = \frac{u_r}{r} \quad (8)$$

$$\epsilon_{zz} = \frac{\partial u_z}{\partial z} \quad (9)$$

$$\gamma_{rz} = \frac{\partial u_r}{\partial z} + \frac{\partial u_z}{\partial r} \quad (10)$$

10 Unknowns

$$\sigma_{rr}, \sigma_{\theta\theta}, \sigma_{zz}, \tau_{rz}, \epsilon_{rr}, \epsilon_{\theta\theta}, \epsilon_{zz}, \gamma_{rz}, u_r, u_z$$

$$c_{11}\frac{\partial^2 u_r}{\partial r^2} - c_{11}\alpha_{rr}\frac{\partial \Delta T}{\partial r} - c_{11}\frac{\partial S_{rr}}{\partial r} + c_{12}\frac{\partial}{\partial r}\left(\frac{u_r}{r}\right) - c_{12}\alpha_{\theta\theta}\frac{\partial \Delta T}{\partial r} - c_{12}\frac{\partial S_{\theta\theta}}{\partial r} + c_{13}\frac{\partial}{\partial r}\left(\frac{\partial u_z}{\partial z}\right) - c_{13}\alpha_{zz}\frac{\partial \Delta T}{\partial r} - c_{13}\frac{\partial S_{zz}}{\partial r} + c_{44}\left(\frac{\partial^2 u_r}{\partial z^2} + \frac{\partial^2 u_z}{\partial r \partial z}\right) + \frac{c_{11} - c_{21}}{r}\left[\frac{\partial u_r}{\partial r} - (\alpha_{rr}\Delta T + S_{rr})\right] + \frac{c_{12} - c_{22}}{r}\left[\frac{u_r}{r} - (\alpha_{\theta\theta}\Delta T + S_{\theta\theta})\right] + \frac{c_{13} - c_{23}}{r}\left[\frac{\partial u_z}{\partial z} - (\alpha_{zz}\Delta T + S_{zz})\right] = 0$$

The displacement formulation of governing equations

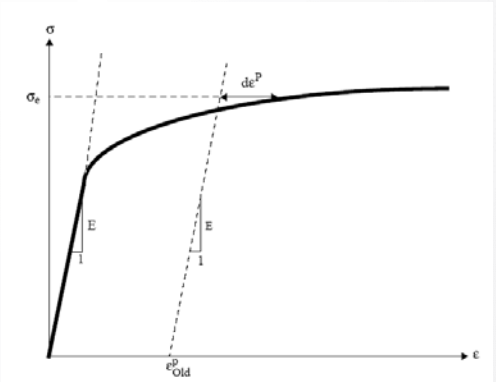

Prandtl-Reuss flow rule for zirconium-based alloy

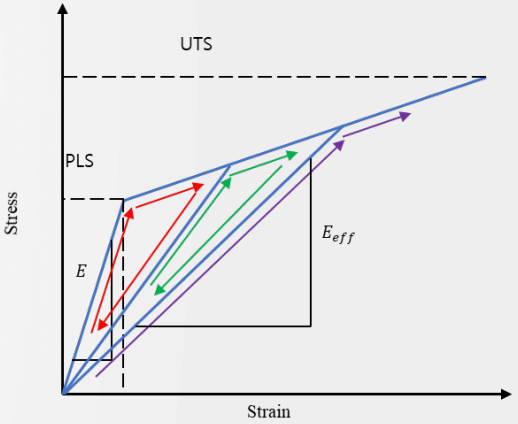

Pseudo-ductile behavior for ceramic composites

Material-dependent plasticity model

Boundary conditions & Differentiation

Code development

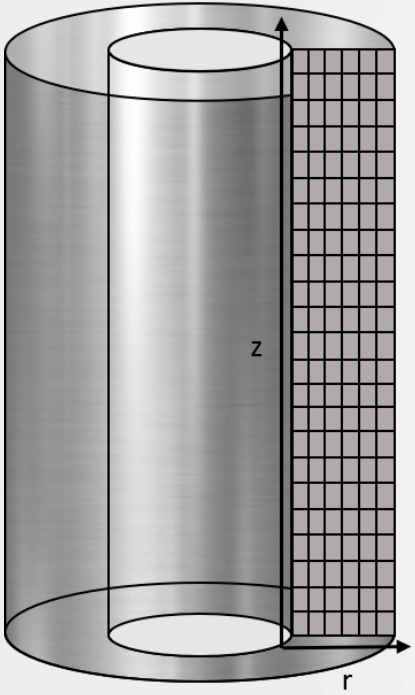

2D (axis-symmetric) full length fuel rod

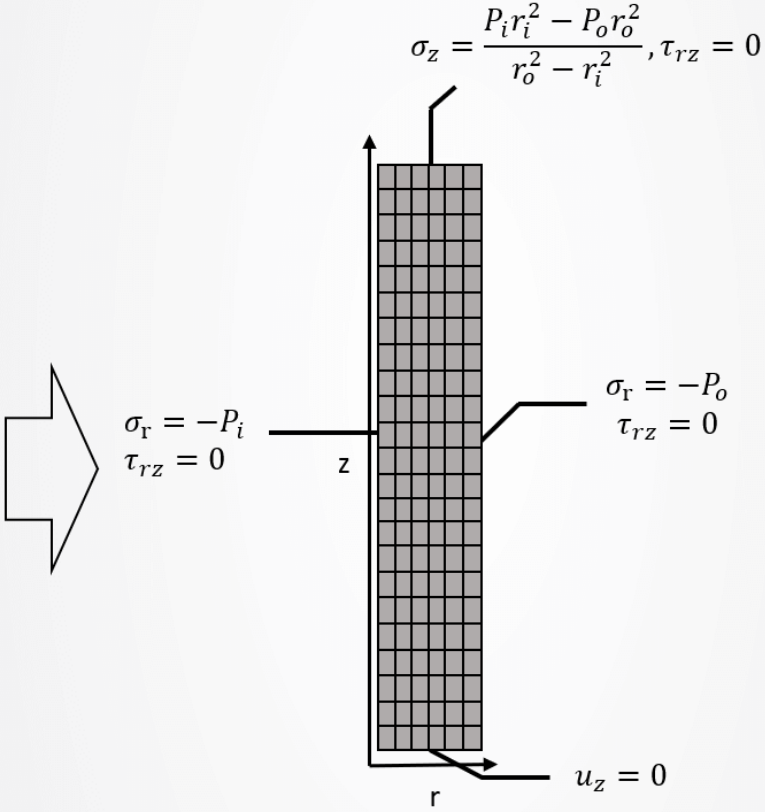

Boundary conditions

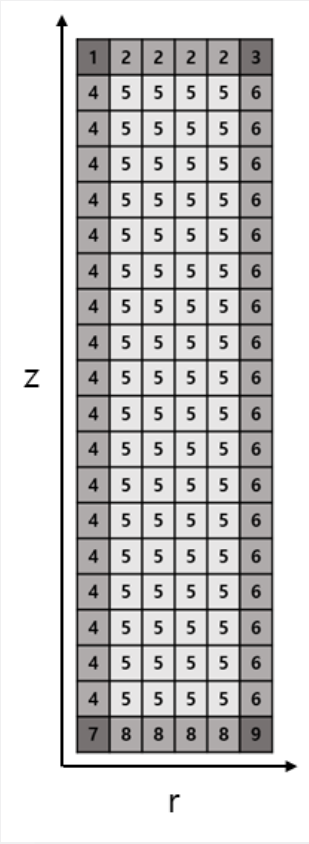

Verification

Code development

Table. Material properties

Material 1			Material 2		
E (Gpa)	ν	$\alpha(K^{-1})$	E (Gpa)	ν	$\alpha(K^{-1})$
460	0.21	4.66×10^{-6}	200	0.3	1.2×10^{-5}

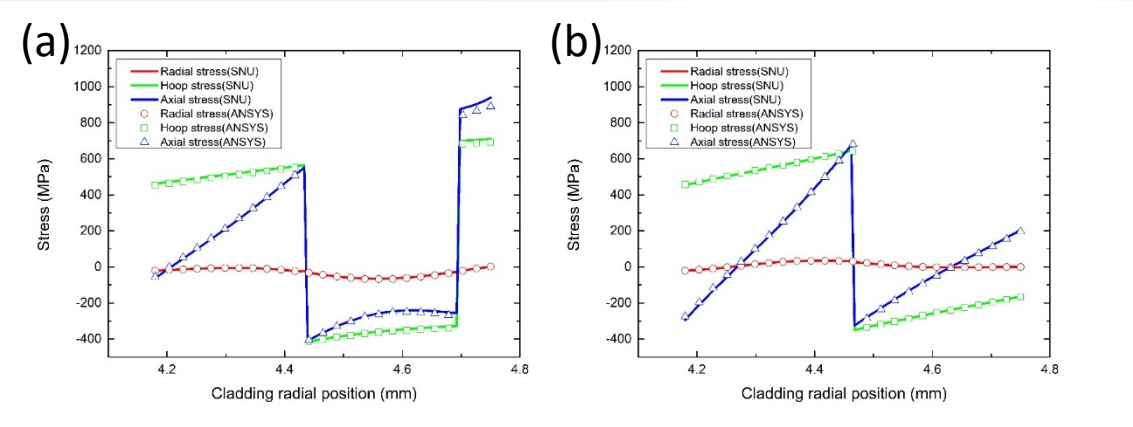

Fig. Stress profile comparison of (a) triple-layer (Material 1 : Material 2 : Material 1 = 0.45 : 0.45 : 0.1) and (b) double-layer (Material 1 : Material 2 = 0.5 : 0.5) : $r_{in} = 4.18\,mm, r_{out} = 4.75\,mm, height = 0.57\,mm, P_{in} = 20\,MPa, P_{out} = 1\,MPa, q' = 18\,kW/m$, $T_{surface} = 340°C$

Table. Material properties

Material		
E (Gpa)	ν	$\alpha(K^{-1})$
99.3	0.37	6×10^{-6}

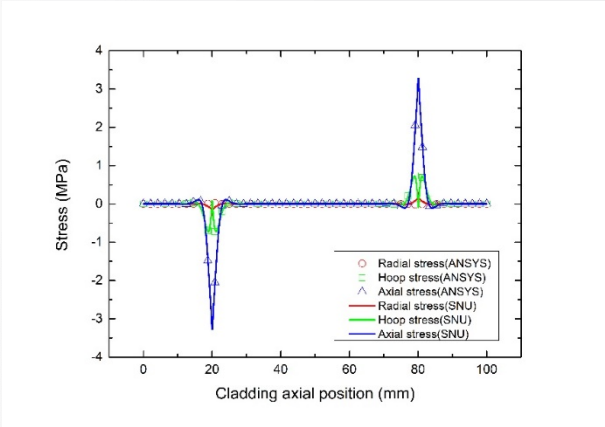

Fig. Stress profile comparison of single-layer : $r_{in} = 4.18\,mm, r_{out} = 4.75\,mm,\ height = 10\,cm, P_{in} = 0\,MPa, P_{out} = 0\,MPa, T_{bottom} = 300°C, T_{top} = 800°C$

Plastic & creep model

Code development

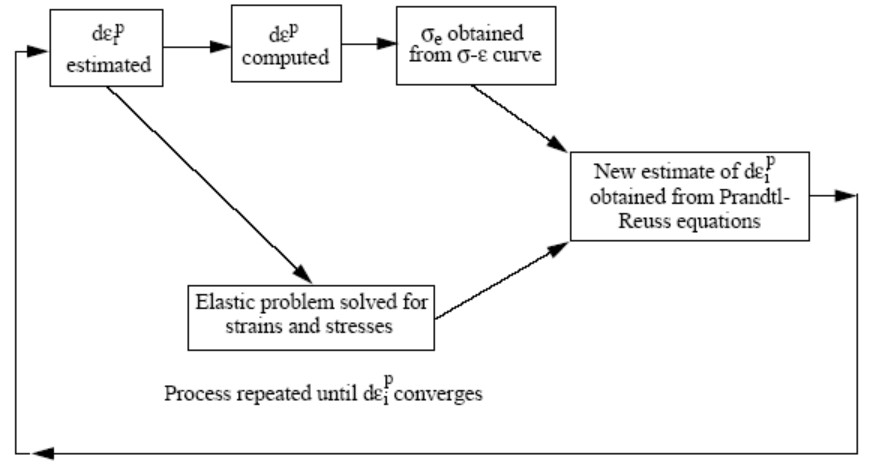

Flowchart of the plastic model of FRAPCON

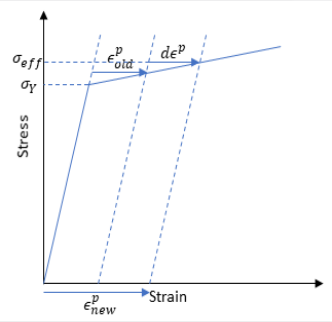

Calculation of Effective Stress(σ_{eff}) from $d\epsilon^p$

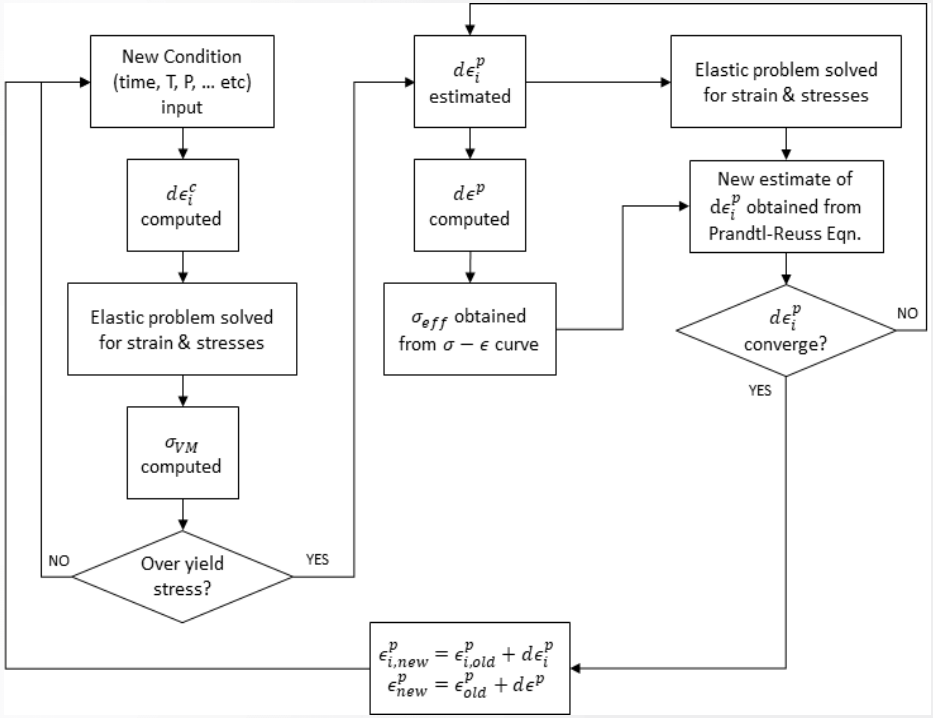

Flowchart of the plastic & creep model of developed code

Model simulation

Code development

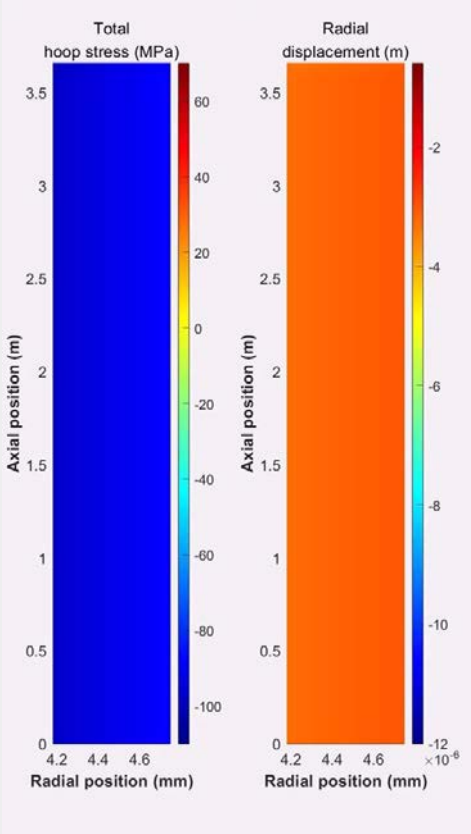

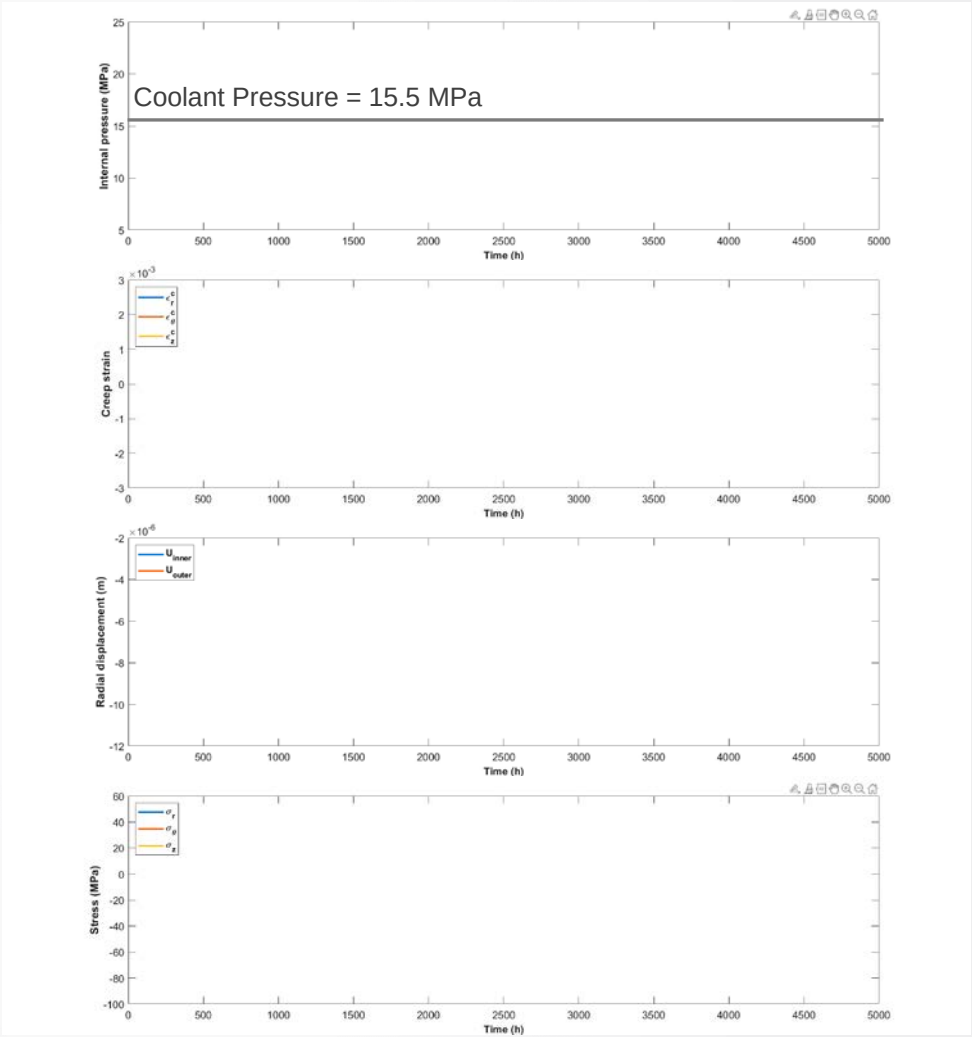

Application of developed code to SiC cladding

- Precedent researches
- Material properties
- MARS code coupling
- Pseudo-ductility
- Failure models
- Steady state analysis
- LBLOCA analysis

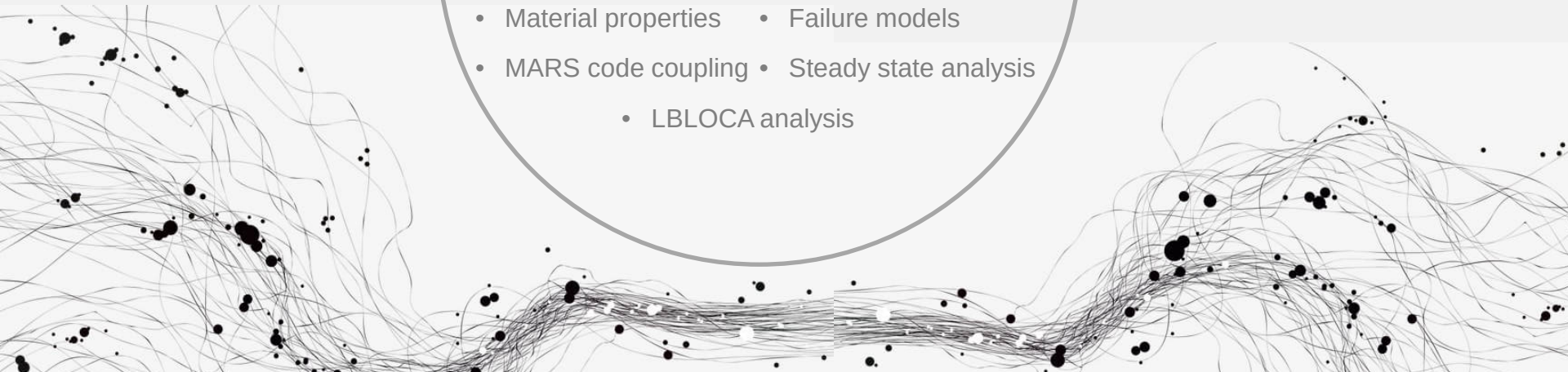

Precedent researches

Application of developed code to SiC cladding

Table. Characteristics of precedent researches and this study

Study	1D/2D	Full-rod scale	Accident analysis	Weibull failure model	Pseudo-ductility	Single/multi layer
Ben-Belgacem (2014) [1]	1D	O	X	X	X	Single
Lee (2015) [2]	1D	O	X	O	X	Single, multi
Stone (2015) [3]	1D	O	X	O	O	Single, multi
Avincola (2016) [4]	2D	X	O	O	X	Multi
Deng (2018) [5]	1D	O	X	O	O	Multi
This study	2D	O	O	O	O	Single, multi

[1] Ben-Belgacem, M., Richet, V., Terrani, K. A., Katoh, Y., & Snead, L. L. (2014). Thermo-mechanical analysis of LWR SiC/SiC composite cladding. Journal of nuclear materials, 447(1-3), 125-142.

[2] Lee, Y., & Kazimi, M. S. (2015). A structural model for multi-layered ceramic cylinders and its application to silicon carbide cladding of light water reactor fuel. Journal of nuclear materials, 458, 87-105.

[3] Stone, J. G., Schleicher, R., Deck, C. P., Jacobsen, G. M., Khalifa, H. E., & Back, C. A. (2015). Stress analysis and probabilistic assessment of multi-layer SiC-based accident tolerant nuclear fuel cladding. Journal of Nuclear Materials, 466, 682-697.

[4] Avincola, V. A., Guenoun, P., & Shirvan, K. (2016). Mechanical performance of SiC three-layer cladding in PWRs. Nuclear Engineering and Design, 310, 280-294.

[5] Deng, Y., Shirvan, K., Wu, Y., & Su, G. (2018). Probabilistic view of SiC/SiC composite cladding failure based on full core thermo-mechanical response. Journal of Nuclear Materials, 507, 24-37.

Pseudo-ductility

Application of developed code on SiC cladding

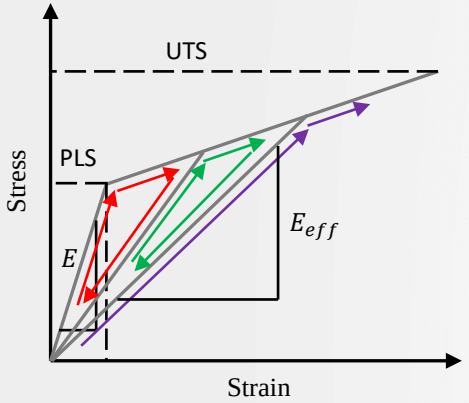

Stress-strain curve of pseudo-ductile material

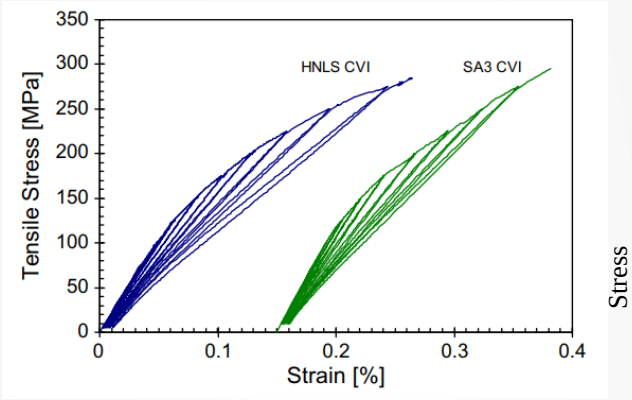

Fig. Typical tensile stress-strain behaviors of Hi-Nicalon Type-S and Tyrano-SA3 composites

Katoh, Y., Snead, L. L., Nozawa, T., Kondo, S., & Busby, J. T. (2010). Thermophysical and mechanical properties of near-stoichiometric fiber CVI SiC/SiC composites after neutron irradiation at elevated temperatures. *Journal of Nuclear Materials*, *403*(1-3), 48-61.

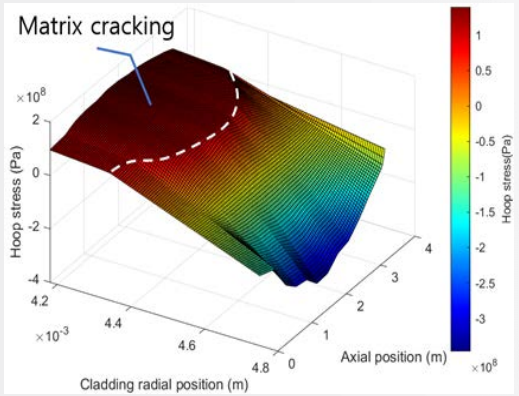

Stress distribution of single-layer SiCf/SiC cladding with pseudo-ductility under shutdown conditions

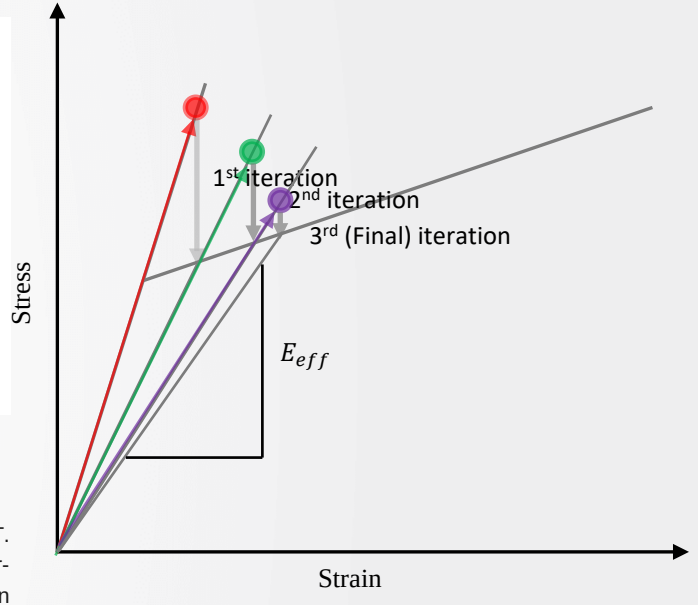

Flowchart of calculating effective Young's modulus

Failure models

Application of developed code on SiC cladding

Weibull Weakest Link Theory (mSiC)

- $P_{s,mSiC}(V) = \exp\left[-\frac{1}{V_0}\int_V \left(\frac{\sigma}{\sigma_0}\right)^m dV\right]$

  V_0 is reference volume, V is specimen volume, σ_0 is scale parameter, m is Weibull modulus, σ is the stress applied to the volume.
- $P_{f,mSiC} = 1 - P_{s,mSiC}$

Failure Criterion (CMC)

- $\frac{\sigma_h^2}{H} + \frac{\sigma_a^2}{A} + \frac{\tau_{ah}^2}{S} = 1, \sigma_h > 0, \sigma_a > 0$

Fitting parameters of failure criterion in axial-hoop stress coordinate system

	H (MPa)	A (MPa)	S (MPa)
PLS	19994	10754	17292
UTS	171810	60172	52441

Shapovalov, K., Jacobsen, G. M., Alva, L., Truesdale, N., Deck, C. P., & Huang, X. (2018). Strength of SiCf-SiCm composite tube under uniaxial and multiaxial loading. Journal of Nuclear Materials, 500, 280-294.

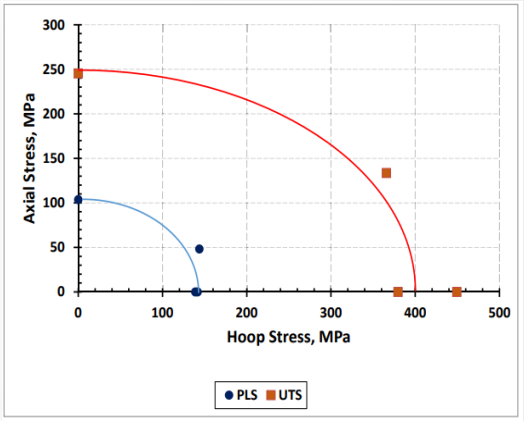

Failure criterion in axial-hoop stress coordinate system

MARS code coupling

Application of developed code on SiC cladding

- For steady state and LBLOCA simulation, the MARS code used in the simulation of Kori Units 3 and 4 was used by modifying the material properties and cladding structure to suit SiC cladding.

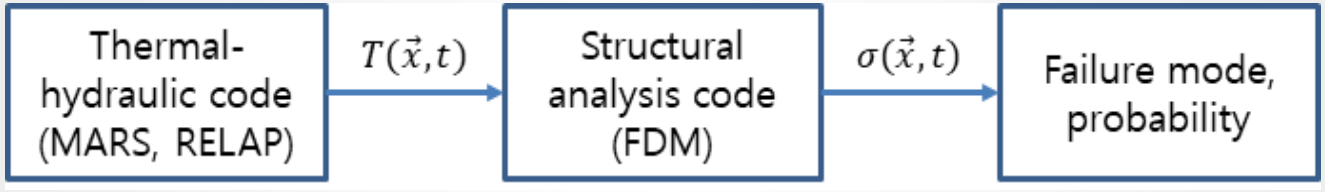

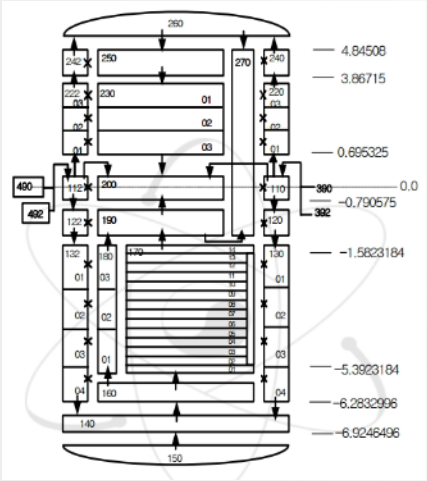

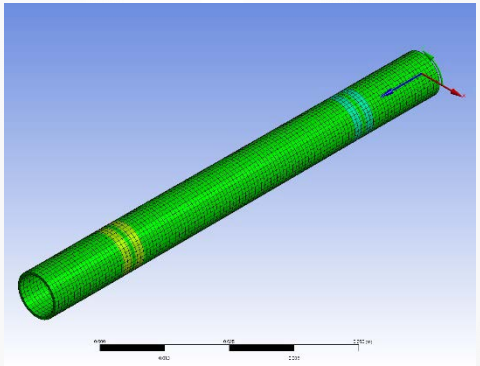

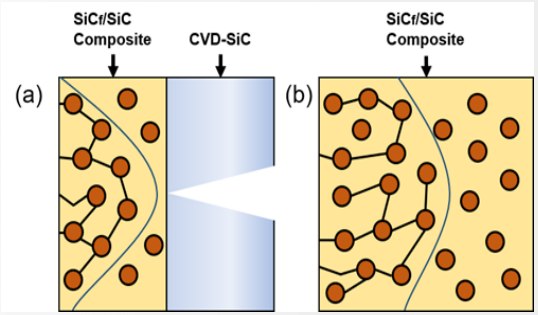

Steady state analysis

Application of developed code on SiC cladding

Shutdown

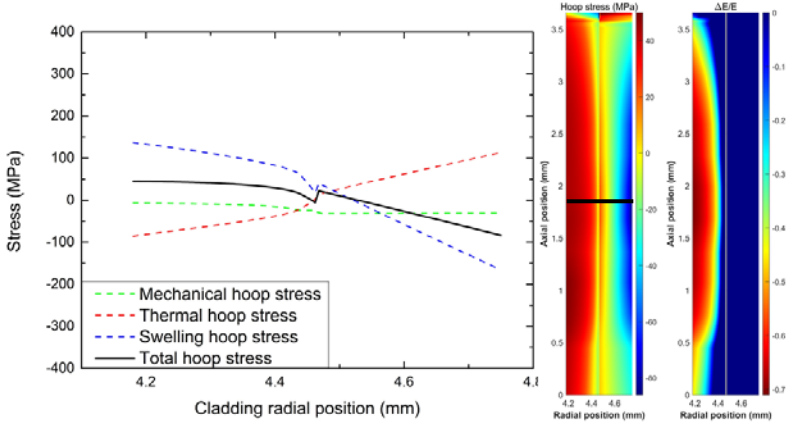

Linear heat rate (kW/m)	17.92
Gap pressure (MPa)	15
Coolant pressure (MPa)	15.5
Failure probability	1.2843e-09

Duplex (SiC_f/SiC-CVD SiC)

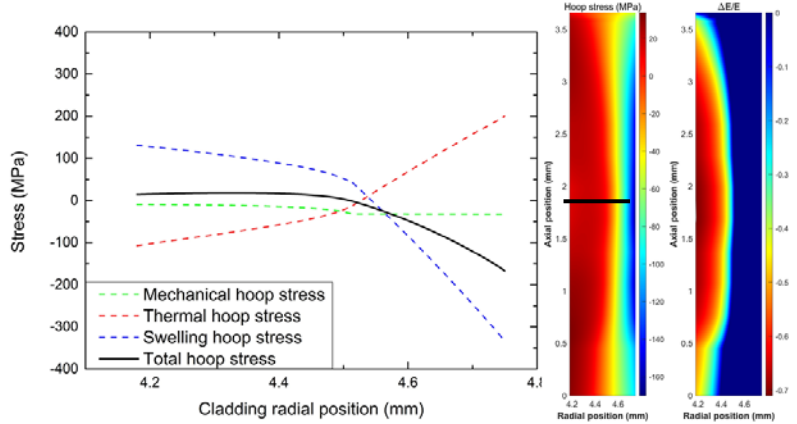

Linear heat rate (kW/m)	17.92
Gap pressure (MPa)	15
Coolant pressure (MPa)	15.5
Failure probability	0

Full composite (SiC_f/SiC)

Steady state analysis

Application of developed code on SiC cladding

- Successfully mitigating the statistical nature of ceramic fractures with composite, both Duplex and full-composite designs show favorable structural integrity expressed by failure probability.

- Full-composite is even considered possible given that the extent of matrix cracking is limited to the half of the cladding thickness.

- If fiber-architecture successfully arrests or blocks cracks of matrix, the full-composite concept can be considered positively.

	Duplex (SiC_f/SiC-CVD SiC)		Full composite (SiC_f/SiC)	
BOL	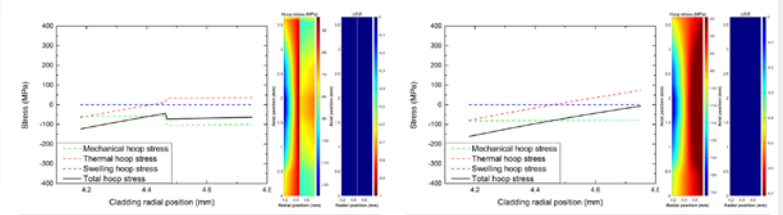			
	Linear heat rate (kW/m)	17.92	Linear heat rate (kW/m)	17.92
	Gap pressure (MPa)	7	Gap pressure (MPa)	7
	Coolant pressure (MPa)	15.5	Coolant pressure (MPa)	15.5
	Failure probability	0	Failure probability	0
shutdown	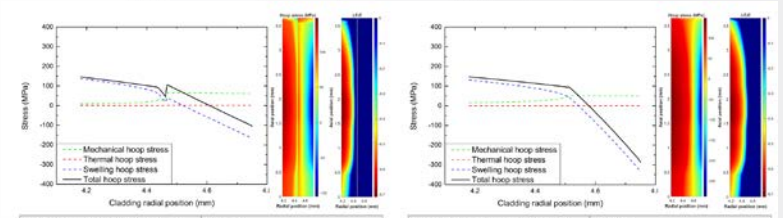			
	Linear heat rate (kW/m)	17.92	Linear heat rate (kW/m)	17.92
	Gap pressure (MPa)	5.5	Gap pressure (MPa)	4.9
	Coolant pressure (MPa)	0.1	Coolant pressure (MPa)	0.1
	Failure probability	0.0192	Failure probability	0
EOL	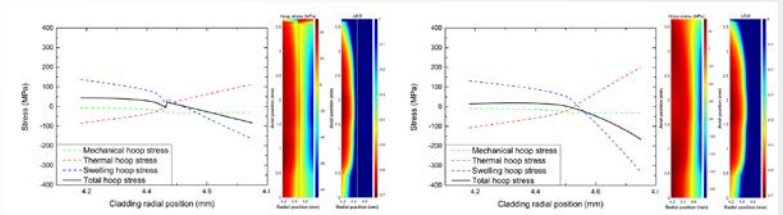			
	Linear heat rate (kW/m)	17.92	Linear heat rate (kW/m)	17.92
	Gap pressure (MPa)	15	Gap pressure (MPa)	15
	Coolant pressure (MPa)	15.5	Coolant pressure (MPa)	15.5
	Failure probability	1.2843e-09	Failure probability	0

LBLOCA analysis - Failure probability

Application of developed code on SiC cladding

Steady state operation

- In the case of multi-layer cladding, no damage shall occur on any floor during steady state operation, and this is defined as P_f.
- This is equal to the multiplication of the probability that each layer survives, so it can be expressed as below.

Survive probability

$$P_f = 1 - \left(1 - P_{f,mSiC}\right) \times \left(1 - P_{f,CMC}\right)$$

($P_{f,mSiC}$ is failure probability of mSiC and $P_{f,CMC}$ is failure probability of CMC)

Accident situation

- In the event of accident, if one layer is broken, the other layer can maintain the geometry of the cladding, and coolable geometry can be maintained.
- So, it is necessary to define the coolable geometry failure probability apart from the failure probability. This can be obtained by multiplying the probability that each layer failures, so it can be expressed as below.

$$P_{f,coolable} = P_{f,mSiC} \times P_{f,CMC}$$

LBLOCA analysis – Duplex SiC cladding

Application of developed code on SiC cladding

- Single-phase
- Nucleate boiling
- Transition boiling
- Film boiling
- Supercritical two-phase or single-phase gas

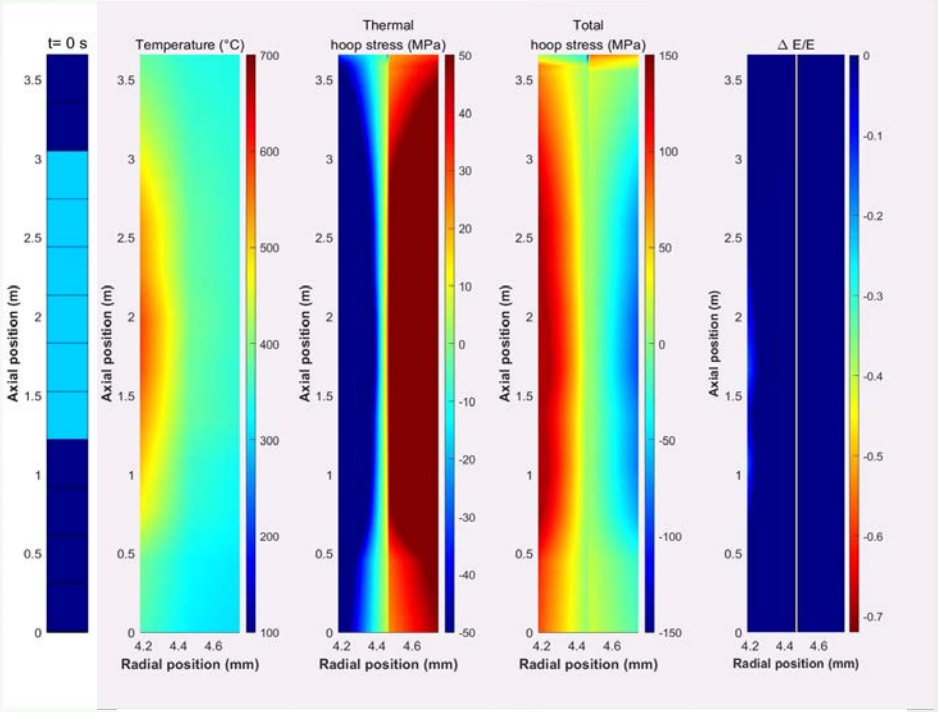

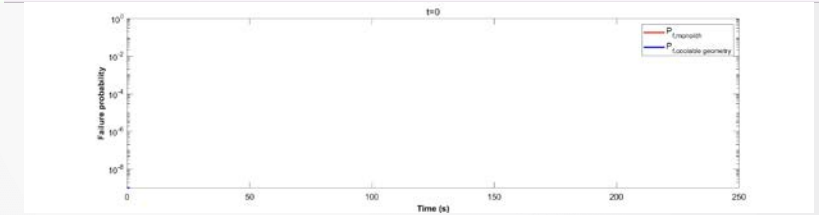

LBLOCA analysis – Full composite SiC cladding

Application of developed code on SiC cladding

- Single-phase
- Nucleate boiling
- Transition boiling
- Film boiling
- Supercritical two-phase or single-phase gas

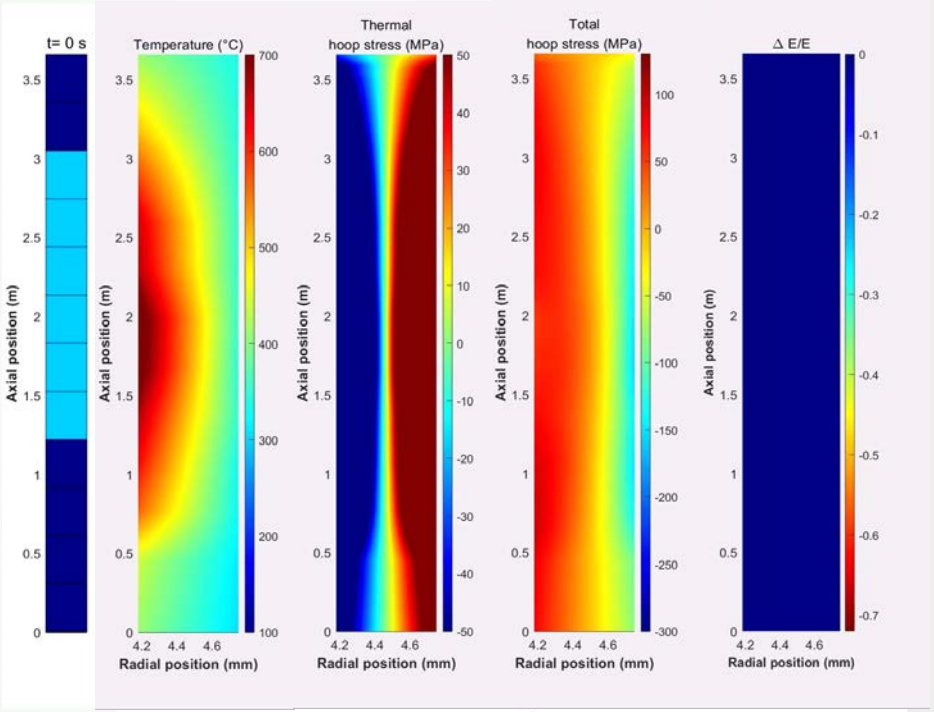

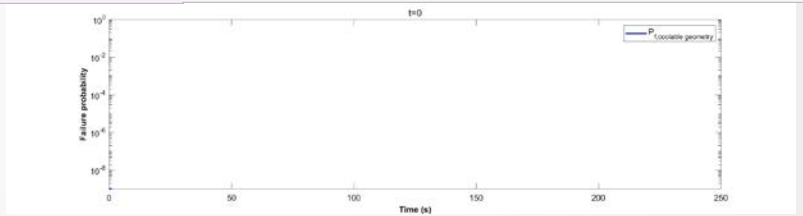

LBLOCA analysis

Application of developed code on SiC cladding

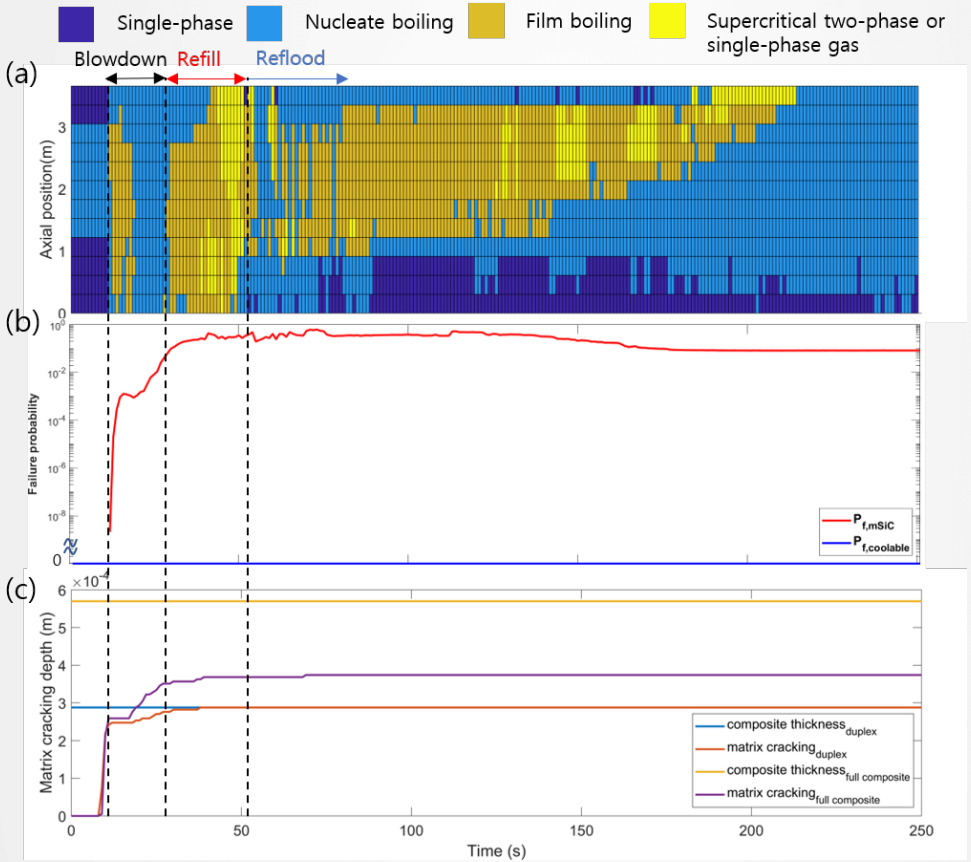

Conclusion

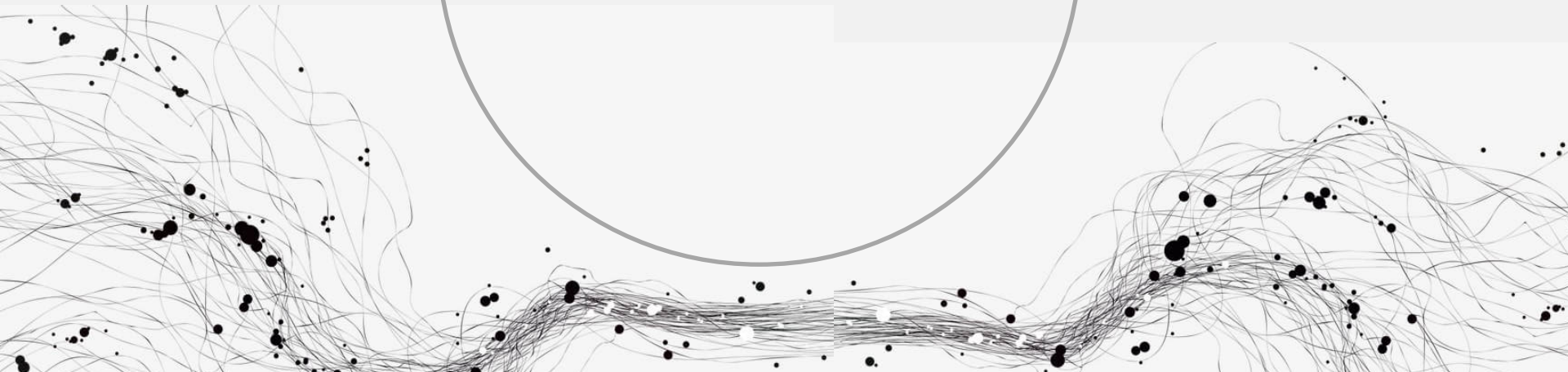

Conclusion

- In normal operation, it is important to find a way to maintain integrity of the cladding in Shutdown.
- In a duplex structure, the outer mSiC layer is likely to be damaged due to tensile stress during LBLOCA.
- Considering that matrix cracking propagates as much as the thickness of the inner CMC layer during LBLOCA in a duplex structure, it is possible to maintain the coolable geometry but not maintain hermiticity.
- In single-layer SiCf/SiC composite structure, matrix cracking propagates less than the cladding thickness and shows low tensile stress due to pseudo-ductility.
- In a single-layer SiCf/SiC composite structure, the outer surface is subjected to weak compressive stress due to swelling. This suggests the possibility of suppressing the propagation of matrix cracks. Thus, the damage to the cladding can be limited and maintain coolable geometry and hermiticity as well.

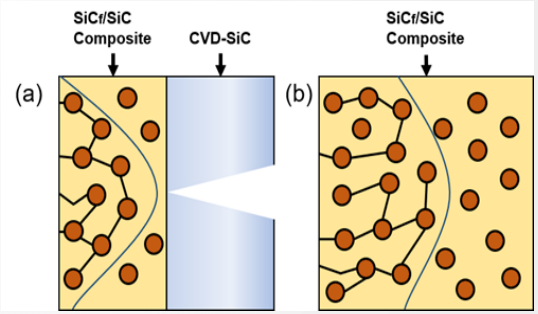

Thank you!

Hyuntaek Rho, Youho Lee*

rho96@snu.ac.kr

leeyouho@snu.ac.kr

Seoul National University

Nuclear Fuel Materials and Safety Laboratory

이 성과는 2020년도 정부(과학기술정보통신부)의 재원으로 한국연구재단의 지원을 받아 수행된 연구임(No. 1711104936)

This work has supported by the National Research Foundation of Korea(NRF) grant funded by the Korea government(MSIT)(No. 1711104936).

Psudo-ductility

Appendix

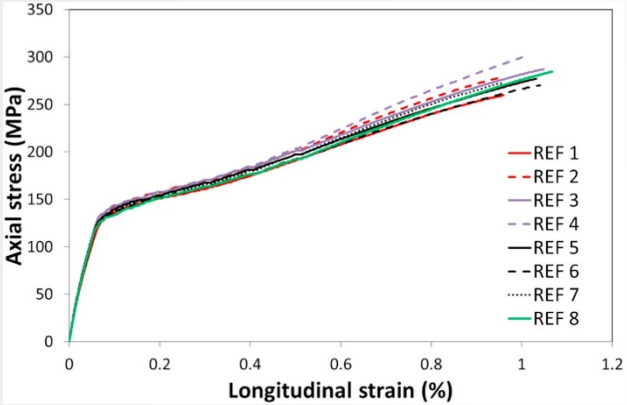

Fig. Tensile stress-strain curves for different tubular SiCf/SiC specimens

Braun, J., Sauder, C., Lamon, J., & Balbaud-Célérier, F. (2019). Influence of an original manufacturing process on the properties and microstructure of SiC/SiC tubular composites. *Composites Part A: Applied Science and Manufacturing*, *123*, 170-179.

	Young's modulus (GPa)	PLS (MPa)	Slope after PLS (GPa)	UTS (MPa)
Axial	173	104	24.3	245(±8)
Hoop	201	93	26.24	400(±11)

Material properties

Appendix

Table. Material properties used in modeling

Properties	Monolithic SiC	SiCf/SiC Composite
Swelling [6]	$S = S_s\left[1 - \exp\left(-\frac{\gamma}{\gamma_c}\right)\right]^{2/3}$ $\gamma_c = -0.57533 + 3.3342 \times 10^{-3}T - 5.3970 \times 10^{-6}T^2 + 2.9754 \times 10^{-9}T^3$ $S_s = 5.8366 \times 10^{-2} - 1.0089 \times 10^{-4}T + 6.9368 \times 10^{-8}T^2 - 1.8152 \times 10^{-11}T^3$ S : swelling, γ : dpa, T : irradiation temperature	The same with mSiC
Thermal conductivity [7]	Non-irradiated : 225 W/mK Irradiated : 12 W/mK	Non-irradiated : 8.5 W/mK Irradiated : 2.4 W/mK
Coefficient of thermal expansion [8]	$\alpha = -0.7765 + 1.4350 \times 10^{-2}T - 1.2209 \times 10^{-5}T^2 + 3.8289 \times 10^{-9}T^3$	The same with mSiC
Elastic properties	E=439.8 Gpa ν=0.114	Next slide

[6] Katoh, Y., Koyanagi, T., McDuffee, J. L., Snead, L. L., & Yueh, K. (2018). Dimensional stability and anisotropy of SiC and SiC-based composites in transition swelling regime. Journal of Nuclear Materials, 499, 471-479.

[7] Katoh, Y., Snead, L. L., Nozawa, T., Kondo, S., & Busby, J. T. (2010). Thermophysical and mechanical properties of near-stoichiometric fiber CVI SiC/SiC composites after neutron irradiation at elevated temperatures. Journal of Nuclear Materials, 403(1-3), 48-61.

[8] Katoh, Y., Ozawa, K., Shih, C., Nozawa, T., Shinavski, R. J., Hasegawa, A., & Snead, L. L. (2014). Continuous SiC fiber, CVI SiC matrix composites for nuclear applications: Properties and irradiation effects. Journal of Nuclear Materials, 448(1-3), 448-476.